



UNIVERSITY OF LEEDS

This is a repository copy of *Effects of synthetic iron and aluminium oxide surface charge and hydrophobicity on the formation of bacterial biofilm*.

White Rose Research Online URL for this paper:  
<http://eprints.whiterose.ac.uk/115591/>

Version: Accepted Version

---

**Article:**

Pouran, HM, Banwart, SA [orcid.org/0000-0001-7223-6678](https://orcid.org/0000-0001-7223-6678) and Romero-Gonzalez, M (2017) Effects of synthetic iron and aluminium oxide surface charge and hydrophobicity on the formation of bacterial biofilm. *Environmental Science: Processes and Impacts*, 19 (4). pp. 622-634. ISSN 2050-7887

<https://doi.org/10.1039/C6EM00666C>

---

© The Royal Society of Chemistry 2017. This is an author produced version of a paper published in *Environmental Science: Processes and Impacts*. Uploaded in accordance with the publisher's self-archiving policy.

**Reuse**

Unless indicated otherwise, fulltext items are protected by copyright with all rights reserved. The copyright exception in section 29 of the Copyright, Designs and Patents Act 1988 allows the making of a single copy solely for the purpose of non-commercial research or private study within the limits of fair dealing. The publisher or other rights-holder may allow further reproduction and re-use of this version - refer to the White Rose Research Online record for this item. Where records identify the publisher as the copyright holder, users can verify any specific terms of use on the publisher's website.

**Takedown**

If you consider content in White Rose Research Online to be in breach of UK law, please notify us by emailing [eprints@whiterose.ac.uk](mailto:eprints@whiterose.ac.uk) including the URL of the record and the reason for the withdrawal request.



[eprints@whiterose.ac.uk](mailto:eprints@whiterose.ac.uk)  
<https://eprints.whiterose.ac.uk/>

1 **Effects of synthetic iron and aluminium oxide surface charge**  
2 **and hydrophobicity on the formation of bacterial biofilm**

3  
4 Hamid M. Pouran<sup>\*a</sup>, Steve A. Banwart<sup>b</sup>, Maria Romero-Gonzalez<sup>c</sup>

5  
6 *<sup>a</sup> LMEI, SOAS, University of London, UK, <sup>b</sup> School of Earth and Environment, University of*  
7 *Leeds, UK, <sup>c</sup> Department of Geography, University of Sheffield, UK*

8  
9  
10 **\*Corresponding author:** Dr Hamid M. Pouran: Tel.: +44 (0)7930 342062

11 Email: [hamidpouran@gmail.com](mailto:hamidpouran@gmail.com)

12

13

14

15

16

17

18

19

20

21

22

23

24

25

26

27

28

29

30

31

32

33

34

35

36

37

38

39

40

1  
2  
3  
4  
5  
6  
7  
8  
9  
10  
11  
12  
13  
14  
15  
16  
17  
18  
19  
20  
21  
22  
23  
24  
25  
26  
27  
28  
29  
30  
31  
32  
33  
34  
35  
36  
37  
38  
39  
40  
41  
42  
43  
44  
45  
46  
47  
48

**Abstract**

In this research, bacterial cell attachments to hematite, goethite and aluminium hydroxide were investigated. The aim was to study the effects of these minerals' hydrophobicity and pH-dependent surface charge on the extent of biofilm formation using six genetically diverse bacterial strains: *Rhodococcus* spp. (RC92 & RC291), *Pseudomonas* spp. (Pse1 & Pse2) and *Sphingomonas* spp. (Sph1 & Sph2), which had been previously isolated from contaminated environments. The surfaces were prepared in a way that was compatible with the naturally occurring coating process in aquifers: deposition of colloidal particles from the aqueous phase. The biofilms were evaluated using a novel, in situ and non-invasive technique developed for this purpose. A manufactured polystyrene 12-well plate was used as the reference surface to be coated with synthesized minerals by deposition of their suspended particles through evaporation.

Planktonic phase growth indicates that it is independent of the surface charge and hydrophobicity of the studied surfaces. The hydrophobic similarities failed to predict biofilm proliferation. Two of the three hydrophilic strains formed extensive biofilms on the minerals. The third one, Sph2, showed anomalies contrary to the expected electrostatic attraction between the minerals and the cell surface. Further research showed how the solution's ionic strength affects Sph2 surface potential and shapes the extent of its biofilm formation; reducing the ionic strength from  $\approx 200$  mM to  $\approx 20$  mM led to a tenfold increase in the number of cells attached to hematite. This study provides a technique to evaluate biofilm formation on metal-oxide surfaces, under well-controlled conditions, using a simple yet reliable method. The findings also highlight that cell numbers in the planktonic phase do not necessarily show the extent of cell attachment, and thorough the physicochemical characterization of bacterial strains, substrata and the aquifer medium are fundamental to successfully implementing any bioremediation projects.

**Keywords:** Interface interactions; Hematite; Goethite; Aluminium hydroxide; Coating; Microorganism; Planktonic growth; Hydrophobicity, Electrostatic interactions; Biofilm formation; Cell adhesion; *Rhodococcus* spp., *Pseudomonas* spp., *Sphingomonas* spp.,

1  
2  
3  
4  
5  
6  
7  
8  
9  
10  
11  
12  
13  
14  
15  
16  
17  
18  
19  
20  
21  
22  
23  
24  
25  
26  
27

## 1. Introduction

Biodegradation, utilizing the capability of microorganisms to transform pollutants into new compounds,<sup>1-3</sup> is a key process in planning management strategies for contaminated soils and aquifers. It is known that in a groundwater environment microbial communities form biofilms, which play a predominant role in the biodegradation process.<sup>1,4</sup>

Bacterial adhesion to metal oxides has been a subject of research for many years, either for its positive effect, e.g. its role in bioremediation, or negative impact on industrial process efficiency, e.g. engineering costs because of biofouling (undesirable growth and accumulation of bacterial cells on the surfaces of engineering structures).<sup>5,6</sup> Although understanding biofilm formation requires a multidisciplinary research approach,<sup>6</sup> we often see that this necessity has been undermined when studying bacterial adhesion on mineral surfaces. Available studies on biofilm formation on metal oxides indicate that the dominant technique to prepare these surfaces is often based on precisely engineered methods, e.g. chemical vapour deposition (CVD).<sup>7,8</sup>

This paper aims to provide a better understanding of biofilm formation via the use of some bacterial strains capable of participating in the bioremediation process on the most common metal-oxide surfaces in aquifers. The results will improve our perception of the interfacial forces governing bacterial cell attachment and our ability to speculate on the extent of biofilm formation and consequently biodegradation efficiency in diverse geological media.<sup>1,3,9-11</sup> It is worth mentioning that biofilm formations using selected model strains have been evaluated in other published studies, namely their attached growth on quartz and polystyrene surfaces.<sup>4,9</sup>

1  
2  
3  
4  
5  
6  
7  
8  
9  
10  
11  
12  
13  
14  
15  
16  
17  
18  
19  
20  
21  
22  
23  
24  
25

Biofilm formation begins with the adhesion of a small quantity of cells.<sup>3,12,13</sup> Figure 1 is a schematic representation of the main steps involved in the biofilm formation process,<sup>13-15</sup> In engineered bioremediation, the traditional assumption is that stimulating a naturally occurring microbial population and/or adding specific microorganisms to a contaminated aquifer will enhance the biodegradation of a targeted compound.<sup>4,14,16</sup> This is based on the concept that deploying these techniques eventually improves biofilm formation and consequently the bioremediation process. For this purpose, planktonic phase growth and variations in cell numbers in this phase are often used to infer bacterial activity, while the success of the bioremediation process depends on effective bacterial colonization and subsequent biofilm formation.<sup>4</sup>

Mineral surface properties can influence both cell attachment and biofilm formation.<sup>4,10,17</sup> The role of surface hydrophobicity and the charge of both the cell surface and the substrate in cell adhesion and attached growth have been studied before and discrepancies between the expected extent of biofilm formation and observed attachment patterns have been found.<sup>4,9,11</sup> This research tests the hypothesis that the surface charge and hydrophobicity of mineral surfaces, specifically metal oxides, determine the extent of biofilm formation. This study differentiates itself from other research by performing tests on metal-oxide surfaces that were synthesized, fully characterized and deposited on reference surfaces in a way compatible with the deposition process that occurs in aquifers,<sup>18-20</sup> e.g. hematite-coated quartz, in contrast to precisely engineered surfaces, e.g. metal-oxide thin films, such as those prepared through chemical vapour deposition (CVD).<sup>10,21,22</sup> Also, this research relies on a novel, in situ and non-invasive technique that uses a water-dipping objective to evaluate biofilm formation on the minerals studied. This imaging method was developed for this study, and it provides a better

1 way to evaluate and quantify biofilms compared to using crystal violet assay, which is a method  
2 frequently used for this purpose.<sup>9</sup>

3 Metal oxides are an important group of soil minerals, in particular because of their wide  
4 presence and the variety of geochemical reactions that occur on their surfaces.<sup>18</sup> Hematite,  
5 goethite and aluminium hydroxide are some of the most common soil minerals, they often  
6 appear in the form of coatings on other mineral surfaces, such as quartz.<sup>10,19,20</sup> In addition, they  
7 have a relatively high point of zero charge (PZC), a specific pH value at which the surface  
8 charge is neutral, which makes their surfaces positively charged in the pH range of natural  
9 environments.<sup>10,18</sup> These metal oxides were selected as model minerals to evaluate the effects  
10 of their surface charge and hydrophobicity on the biofilm formation of specific bacterial strains.  
11 Studying these metal oxides also allows building up a more comprehensive picture of how  
12 complex surfaces, e.g. aluminosilicates and binary metal oxides, can affect attached microbial  
13 growth.

14 Similar to metal oxides, bacterial cells also carry a pH-dependent surface charge at the  
15 cell-water interface.<sup>10,23</sup> This surface charge stems from associated functional groups on the  
16 surface of the cell wall, which through protonation/ deprotonation processes generates a pH-  
17 dependent surface charge.<sup>24,25</sup> Nevertheless, most of the available information indicates that  
18 bacterial surfaces dominantly exhibit an overall negative charge in the pH range of natural  
19 environments.<sup>26-29</sup> Hence, attraction between the opposite surface charges of bacterial cell and  
20 metal-oxide surfaces with pH values like natural environments is expected. Here, we report the  
21 results of studying the biofilm formation of specific environmental isolates on hematite,  
22 goethite and aluminium hydroxide, which was performed under well-controlled experimental  
23 conditions and in a reproducible manner.

24

25

1  
2  
3  
4  
5  
6  
7  
8  
9  
10  
11  
12  
13  
14  
15  
16  
17  
18  
19  
20  
21  
22  
23  
24

## **Experimental section**

### **1. Materials and Methods**

#### **2.1 Chemicals**

In the experiments, certified ACS reagents, chemicals that meet or exceed the latest ACS specifications, were supplied by Fisher Scientific (UK) and used without further purification. Ultra-high quality water (UHQ, conductivity 18.2 MΩ/cm at 25°C) was used throughout the experiments. All chemicals were prepared in Pyrex glass vessels.

#### **2.2 Surface preparation – synthesis, coating and characterization**

Hematite was prepared by heating an acidic solution of FeCl<sub>3</sub>.<sup>10,30</sup> Goethite was synthesized by heating an alkaline solution of Fe(NO<sub>3</sub>)<sub>3</sub> in a polyethylene flask for 60 hours at 70°C.<sup>10,31</sup> The aluminium hydroxide synthesis method was based on adding aluminium nitrate to an alkaline solution.<sup>10,32</sup>

A STOE STADI P X-ray powder diffractometer and a Perkin Elmer Spectrum Spotlight FTIR imaging system for Fourier-transform infrared spectroscopy (FTIR) were used to analyze the synthesized materials. For XRD analysis, copper K alpha was the radiation source; a range of 10–70 degrees and a step size of 0.02 degrees were the test parameters. In FTIR experiments, the spectrum resolution was 4 cm<sup>-1</sup>, covering the range of 4,000-400 cm<sup>-1</sup> wave numbers, and 150 scans were collected for each sample.

To determine the point of zero charge (PZC) of the synthetic metal oxides, potentiometric titration was done. An automated potentiometric titrator (Metrohm, 718 STAT, Titrino) was used. During titrations, acid (HCl, 0.1M) and base (NaOH, 0.1M) were added by a computer-controlled micro-burette with a dispensing volume of 0.01 ml. The titrator was

1 adjusted to add successive acid or base when the absolute value of the potential drift was equal  
2 to or less than 5 mV/min. The sample suspensions were purged with N<sub>2</sub> gas to remove carbon  
3 dioxide from the system for approximately two hours before titration, which was performed in  
4 an N<sub>2</sub> atmosphere.<sup>10</sup> In these tests, a magnetic stirrer provided continuous stirring and the  
5 suspension temperature was kept at 25°C during the titration period. Surface hydrophobic/  
6 hydrophilic properties of the synthetic minerals were obtained by measuring the water-drop  
7 contact angle in air. Contact angles were obtained using the sessile drop method and a KRÜSS  
8 DSA 100 drop-shape analysis system. An aliquote of 3µl of UHQ water was added to the  
9 mineral surfaces at room temperature.<sup>10</sup> The contact angle between the surface and a tangent  
10 drawn on the drop surface, passing through the triple point of atmosphere-liquid-solid, was  
11 measured. Iron and aluminium oxides' hydrophilic nature stems from their surface hydroxyl  
12 groups.<sup>33</sup> In general, surfaces with a water-drop contact angle of less than 90 degrees are  
13 hydrophilic; nevertheless, for the surfaces studied, the expected water-drop contact angles were  
14 considerably less.<sup>34-37</sup> The MATH, Microbial Adhesion to Hydrocarbon Test, is an established  
15 method to quantify microbial cell surface hydrophobicity via their attachment to hydrocarbon  
16 droplets;<sup>38-40</sup> this technique has been performed on selected model strains in other published  
17 studies.

18 The coating process involved the direct deposition of mineral particles from an aqueous  
19 suspension by evaporation, which has been explained in detail in a previous publication.<sup>10</sup>  
20 After this step, the coated polystyrene surfaces were assessed using optical microscopy (Zeiss,  
21 Axiovision), direct imaging and contact-angle measurements to determine their hydrophobicity  
22 (as described above). The ATR-FTIR, attenuated total reflection-Fourier transform infrared,  
23 technique using a Specac Silver Gate Essential Single Reflection ATR System and XPS, and  
24 X-ray photoelectron spectroscopy (KRATOS-Axis 165) were also used to compare the

1 chemical properties of altered surfaces with those of reference polystyrene and mineral  
2 surfaces<sup>10</sup> – please see supporting information (SI).

### 3 **2.3 Bacterial strains, growth conditions and sample preparation**

4 Six bacterial strains were isolated for bacterial-adhesion and attached-growth studies.  
5 *Rhodococcus* spp., RC92 and RC291, both Gram-positive, were isolated from soil samples  
6 from a polluted gasworks site in northeast England. The bacteria *Pseudomonas* spp. (Pse1 and  
7 Pse2) and *Sphingomonas* spp. (Sph1 and Sph2) were isolated from groundwater at a phenol-  
8 contaminated site in the West Midlands (England). The strains Pse1, Pse2, Sph1 and Sph2 are  
9 Gram-negative. They have been classified using comparative 16S rRNA sequencing.<sup>4,9</sup> All  
10 strains were maintained on a solid R2A medium (Oxoid).<sup>41</sup>

11 The bacterial strains were grown in an AB10 medium,<sup>42</sup> which is a defined medium  
12 with known exact chemical composition – please see supporting information (SI). The carbon  
13 source was 2 mM of glucose, and the incubation time was 96 hours at 20°C on a shaker at 150  
14 rpm. After incubation, cells were harvested by centrifugation in an early stationary phase and  
15 washed in 10 ml of sterile 0.9% NaCl solution. Samples of washed and resuspended strains (in  
16 0.9% NaCl), with an optical density (OD) of 0.01 at  $\lambda = 600$  nm, were resuspended in the AB10  
17 medium with different carbon-source treatments. Two variations of carbon sources, 2 mM of  
18 glucose and 2 mM of potassium acetate (KAc), were used to evaluate whether there was a  
19 difference between these two carbon sources in the extent of biofilm formation; in addition,  
20 the same medium with no carbon source was used as a control. Previous studies indicate that  
21 these environmental isolates can metabolize glucose and potassium acetate, and similar growth  
22 media have been used in the past to study biofilm formation on model substrata with different  
23 surface properties.<sup>4,9</sup> The aim of this study was to perform experiments, including bacterial  
24 cell growth and attachment, in a well-controlled environment. A similar incubation method and  
25 growth medium (defined medium AB10<sup>42</sup>), in addition to studying the attachment

1 morphologies of these individual environmental isolates to polystyrene, have been reported in  
2 other publications; <sup>1,4,9-11,43,44</sup> these were used to cross-compare with this research. Extending  
3 this study to conditions more compatible with natural environments should be part of future  
4 studies.

5

## 6 **2.4 Biofilm formation studies**

7 Six strains, four different surfaces, two carbon sources and one experimental control  
8 (AB10 medium with no carbon source) were analyzed in triplicate to assay biofilm formation  
9 for a total of 216 samples. In these experiments, reference polystyrene plates were prepacked  
10 and radiation-sterilized. The mineral-coated polystyrene plates <sup>10</sup> were sterilized by immersion  
11 in a 70% ethanol medium for one hour prior to incubation and dried under aseptic conditions  
12 in a laminar flow cabinet.

13 Non-invasive, in situ direct imaging using Syto9 stain (green fluorescent nucleic acid  
14 stain, supplied by Invitrogen) was used as the primary technique to assay biofilm. <sup>45,46</sup> The  
15 reference polystyrene and metal-oxide coated polystyrene well-plates, each with 12 wells and  
16 a nominal culture area of 3.82 cm<sup>2</sup> for each well, <sup>47</sup> were used as substrata for biofilm formation  
17 studies. Samples of bacteria suspension were prepared at an optical density (OD) of 0.01 at  $\lambda$   
18 = 600 nm using AB10 medium, pH $\approx$  6.5, with glucose, potassium acetate and no carbon source.  
19 Then, 2 ml of prepared medium was added to each micro-well. The 12 well-plates were  
20 incubated for 96 hours at 20°C (Fig. 2); then, 200  $\mu$ l of each of the bacterial samples, from  
21 their planktonic phase, was transferred to a 96-micro well-plate and the OD was measured at  
22  $\lambda=630$  nm to determine planktonic phase growth. To assess the planktonic phase of individual  
23 environmental isolates, the measured optical density (OD) at  $\lambda= 630$  nm was calibrated against  
24 the number of colony-forming units (CFU) for each strain. This calibration was used to  
25 compare growth in the planktonic phase for each individual strain. The rest of the planktonic

1 phase was discarded and each well was gently washed three times by adding 5ml of 0.9% sterile  
2 NaCl solution that was slowly added to the well wall and bottom intersection, using a pipette  
3 tip, to remove cells in the planktonic phase and ensure that only bacterial cells which had  
4 attached to the surface were present.

5 Each well of the reference polystyrene and coated plates was stained by adding 0.5 ml  
6 of Syto 9, which was diluted 500x. The thickness of the added stain layer that formed on the  
7 bottom of the well was approximately 1.25 mm (the surface area of each well was 3.82 cm<sup>2</sup>).  
8 The stained wells were directly imaged in situ using a 100x magnification Zeiss Achroplan  
9 water-dipping objective (Fig. 2). For imaging, a Zeiss AxioVision epifluorescence microscope  
10 with automated Z-height focusing (Z-stacking) was used for extended depth and field imaging.  
11 With this technique a series of images are acquired at different focus positions, which allows  
12 imaging through a thick section or of a rough surface (Fig. 2). Images were captured with an  
13 AxioCam black & white camera using a 450-490 nm narrow-band pass filter. For each sample,  
14 15 images were captured and then analyzed using AxioVision 4.6 and Image J software. From  
15 these digital images, direct cell counts were obtained and reported as cells/cm<sup>2</sup> (since each  
16 experiment was conducted in triplicate, each data point represents an average of 45 data points).  
17 The microscope water-dipping objective had restricted lateral motion, due to the well's sides,  
18 which confined the imaging area (Fig. 2). Images to study bacterial cell attachment on the  
19 substrate, at the bottom of each well, were taken from a circular accessible surface with a  
20 diameter of 11mm located at the centre of the wells. As mentioned earlier, microscope Z-  
21 stacking provided the option of acquiring images at different focus positions. This technique  
22 was used to determine biofilm depth when the cells had formed dense biofilms.

23

## 24 **3. Results and Discussion**

### 25 **3.1 Surface coating and characterization**

1  
2  
3  
4  
5  
6  
7  
8  
9  
10  
11  
12  
13  
14  
15  
16  
17  
18  
19  
20  
21  
22  
23  
24  
25

XRD and FTIR analysis showed that the synthetic materials matched the expected metal oxides. Detailed surface analysis, including ATR-FTIR, XPS and water-drop contact angle measurements, confirmed the compatibility of the coated reference plate's surface properties with pure mineral phases<sup>10</sup> – please see supporting information (SI) section.

Mineral surfaces' PZC was obtained at the common intersection point of more than one potentiometric titration curve at different ionic strengths. The PZC of polystyrene was considered to be neutral.<sup>4</sup> The PZC for hematite, goethite and aluminum hydroxide was 7.5, 8.5 and 8.9, respectively, indicating a positive charge on the surface at the pH of the adhesion experiments. The contact angle values for polystyrene (90°) and hematite ( $\approx 45^\circ$ ) demonstrate that both surfaces are hydrophobic. In the case of goethite and aluminium hydroxide, the contact angle value was lower than 10°, indicating that these surfaces are hydrophilic;<sup>10</sup> – for further details and related images please see supporting information (SI) section.

The relative hydrophobicity of the bacterial species studied in this research has been determined before in independent experiments<sup>1,4,9</sup> that suggest that RC92, RC291 and Sph1 are hydrophobic, while Pse1, Pse2 and Sph2 are hydrophilic strains, after incubation in both AB10 with glucose and potassium acetate carbon sources.

The PZC of bacterial cells is typically between 3.5 and 5.0.<sup>5,10,23,24,48</sup> Since the pH of the experiments, approximately 6.5, was higher than the environmental isolates' expected PZC, the overall surface charge of the cells was anticipated to be negative under the experiment's conditions.

With respect to hydrophobicity, RC92, RC291 and Sph1 were hydrophobic, like the reference polystyrene surface, while Pse1, Pse2 and Sph2 were hydrophilic, similar to the hematite, goethite and aluminium hydroxide coated well-plates. Considering electrostatic interactions, the PZC values of the bacterial strains and the metal oxide surfaces were,

1 respectively, below and above the experiments' pH (6.5); therefore, electrostatic attraction was  
2 expected to drive cell adhesion and subsequent biofilm growth on the mineral surfaces.

3

### 4 **3.2 Biofilm studies**

5 Figure 3. shows the total number of cells calculated in the planktonic phase for the  
6 studied strains and surfaces. These data relate to the growth medium, AB10, when glucose was  
7 the carbon source. As seen in the planktonic phase cell numbers, for each strain, these were  
8 within the same range and compatible, regardless of the study surface. Similar patterns were  
9 observed when the AB10 carbon source was potassium acetate (KAc) – please see supporting  
10 information (SI). The bacterial strains did not grow on the AB10 medium with no added carbon  
11 source. The results suggest that the strains thrive better in a medium with a glucose carbon  
12 source compared to potassium acetate. More importantly, the level of cell growth in the  
13 planktonic phase seems to be independent of the surface charge and hydrophobicity of the  
14 growing environment's surface. As Figure 3 indicates, the numbers of RC92 and RC291,  
15 *Rhodococcus* spp., in the planktonic phase are less than *Pseudomonas* spp. (Pse1 & Pse2), and  
16 *Sphingomonas* spp. (Sph1 & Sph2). This can be attributed to the surface properties of the  
17 *Rhodococcus* species that encourage cell aggregation in an aqueous medium.<sup>49,50</sup> Prior to  
18 measuring the planktonic phase, the samples were vortexed to disperse flocs of these strains.

19 Based on the hydrophobic properties of the cells and surfaces, the expected pattern is  
20 to see more cell attachment of the hydrophobic strains, RC92, RC91 and Sph1, on polystyrene,  
21 and more biofilm on the hydrophilic reference mineral surfaces formed by Pse1, Pse2 and  
22 Sph2.

23 Figures 4–6 show the bacterial strain adhesion patterns of the reference polystyrene and  
24 mineral surfaces in the AB10 medium with a glucose carbon source. The biofilms formed on

1 polystyrene are similar to those previously reported in other research, using the same variables.

2 4.9

3 RC92 had overall poor attachment on the studied surfaces. The attached growth  
4 colonies of this strain on the reference polystyrene formed different groups of cells that aligned  
5 to shape and split and relatively short chain-type cell arrangements, while for the mineral  
6 surfaces attached individual and separated cells were observed (Figs 4a–4d). RC291 is a Gram-  
7 positive, hydrophobic bacterial strain like RC92, with comparable attachment morphologies  
8 for minerals, but different colony forms on the reference polystyrene surface. As shown in  
9 Figure 4h, RC291 forms proliferated, with dense and highly structured biofilm on the reference  
10 polystyrene.

11 Pse1 and Pse2 are Gram-negative and hydrophilic. As seen in Figure 5 (a–d), Pse1  
12 forms cell clusters on all surfaces; however, the numbers and sizes of these clusters are  
13 considerably higher for biofilms attached to metal oxides. The biofilms on polystyrene are  
14 sparse and shape small micro-colonies (Fig. 5d), while they are notably denser on mineral  
15 surfaces. Pse2 shows the same biofilm formation phenotype on metal oxides, Figure 5 (e–g),  
16 but for the polystyrene the attached cells are more aggregated and show discrete micro-colonies  
17 (Fig. 5h).

18 In these experiments, Sph1 was the only Gram-negative strain with hydrophobic  
19 surface properties. As Figure 6 (a–c) displays, Sph1 cells attached to mineral surfaces show  
20 poor adhesion, while biofilms formed on reference polystyrene are extensive and abundant  
21 (Fig. 6d). Sph2 is a Gram-negative strain with hydrophilic surface properties. Negligible  
22 attachment to metal oxide surfaces (Fig. 6 e–g), in contrast to the notable biofilm formation on  
23 reference polystyrene, compatible with Sph1, was the dominant morphology for attached cells.  
24 The results are striking, as hydrophobic Sph1 and hydrophilic Sph2 show matching biofilm

1 formation patterns on the studied surfaces. Table 1 summarizes the biofilm morphologies of  
2 attached cells on the studied mineral and polystyrene surfaces.

3 The observed morphologies for attached cells using KAc as the carbon source were  
4 similar to AB10 with glucose – please supporting information (SI) for details.

5 Figure 7 shows the numbers of attached cells based on a direct count of cell numbers  
6 from captured images. As seen, Pse1 and Pse2 are the strains with the highest numbers of  
7 attached cells to metal oxides. The cell numbers for RC92 and RC291 are significantly higher  
8 for the reference polystyrene compared to mineral surfaces. Similarly, the numbers of Sph1  
9 and Sph2 attached cells are notably higher for the reference polystyrene compared to the metal  
10 oxides.

11 Comparing the numbers of attached cells on the studied surfaces (Fig. 7) with their  
12 respective planktonic phase growth (Fig. 3) suggests that a high number of cells in the  
13 planktonic phase does not necessarily correspond to extensive cell attachment and biofilm  
14 formation.

15 The hydrophobic nature of the *Rhodococcus* strains, RC92 and RC291, is a likely  
16 reason for their negligible attachment to hydrophilic minerals. Nevertheless, hydrophobicity  
17 does not fully explain their attachment pattern to the hydrophobic reference polystyrene surface  
18 and the clear differences in biofilm morphology seen between these two strains (Figs 6 d, h).  
19 A previous study<sup>4</sup> suggests that lipophilic macromolecules of RC92 and RC291 cell walls play  
20 a key role in their attachment to hydrophobic polystyrene surfaces. These macromolecules  
21 associate differently with cells, which consequently influences cell attachment and biofilm  
22 proliferation on hydrophobic surfaces. For RC291, polar and non-polar lipids are closely  
23 associated with the cells that facilitate cell attachment to hydrophobic surfaces and cell-cell  
24 interactions. In contrast, although RC92 produces large numbers of diverse extracellular  
25 lipophilic molecules, these materials are not closely associated with the cells and can be

1 detached and released to the medium. Therefore, the ability to retain extracellular lipophilic  
2 materials is a likely element that shapes the attachment phenotypes of RC92 and RC291.<sup>4</sup>

3 Pse1 and Pse2, despite similarities in their genetics, attach differently to polystyrene.  
4 They show similar attachment morphologies, but the number of cells attached to the  
5 polystyrene surface is notably higher for Pse1. The difference in the extent of attachment to the  
6 studied surfaces, and the considerable biofilm formation of these hydrophilic strains on the  
7 hydrophobic polystyrene surface, can be attributed to their specific physiological features.<sup>51</sup>  
8 Other studies,<sup>4,44</sup> using microscopic and spectroscopic analyses in addition to studying cell  
9 attachments under treatment with D-NaseI, have revealed that for the *Pseudomonas* species the  
10 extracellular DNA (eDNA) determines the difference between Pse1 and Pse2 attachment  
11 patterns. The presence of eDNA enhances Pse1 adhesion to a hydrophobic surface.

12 The *Sphingomonas* strains' adhesion patterns to hydrophobic polystyrene and  
13 hydrophilic mineral surfaces are compatible. The *Sphingomonas* species has Gram-negative  
14 strains, these are unique compared to other Gram-negatives. Instead of lipopolysaccharide  
15 (LPS) *Sphingomonaceae spp.*, bacterial strains have glycosphingolipids (GSL), which are a  
16 subgroup of glycolipids (lipids that are linked to a carbohydrate chain). They contain the  
17 sphingosine, an amino alcohol, moiety. These chemical structures are amphiphilic, having both  
18 hydrophobic and hydrophilic parts, the molecules generally have similarities to the  
19 physicochemical and functional properties of lipopolysaccharides.<sup>52,53</sup> The amphiphilic  
20 characteristi of these *Sphingomonas spp.* Cell-surface molecules can probably facilitate the  
21 attachment of these strains to both hydrophobic and hydrophilic surfaces. Similar biofilm  
22 formation patterns of Sph2 on a polystyrene surface have been reported before.<sup>4,9</sup> However,  
23 this characteristic does not explain the poor Sph2 attachment to mineral surfaces. The  
24 polystyrene surface charge is neutral,<sup>10</sup> so electrostatic interactions can only play a negligible  
25 role in Sph2 attachment to this surface. Unlike hydrophobic polystyrene, mineral surfaces are

1 hydrophilic with a positive surface charge <sup>10</sup> in pH of the experiment. The expected PZC of  
2 Sph2 under the experimental condition, pH 6.5, is negative and attractive cell-mineral  
3 electrostatic interaction is anticipated to support cell attachment and biofilm formation. This is  
4 contrary to the observed pattern. To investigate these discrepancies further, additional  
5 experiments were performed to determine if medium ionic strength affects the electrostatic  
6 interactions between two hydrophilic entities.

7 Sph2 zeta potential was measured using a zeta potential analyzer (Zeta Plus, Brookhaven  
8 Instruments, Huntsville, NY). Zeta potential can be defined as the electrical potential difference  
9 when there is interference between a bulk aqueous medium and a static fluid attached to a  
10 bacterial cell. <sup>54</sup>

11 Figure 8a shows zeta potential values for a Sph2 strain suspended in 1 mM of KCl. As  
12 can be seen, this bacterial strain shows negative surface potential at circa neutral pH values.  
13 This agrees with previously published research indicating that bacterial cells often have a  
14 relatively low PZC and carry a negative surface charge in natural media. <sup>5,10,23,24,48</sup>  
15 Nevertheless, this result cannot explain the attachment behaviour of Sph2 on positively charged  
16 metal-oxide surfaces.

17 In this research, cell attachments were evaluated after 96 hours of incubation. During  
18 this time, bacterial cells, immersed in an AB10 medium, were exposed to metal oxides and  
19 polystyrene surfaces. To evaluate the effect of incubation time on cell surface charge, Sph2  
20 cells were harvested from the planktonic phase of hematite plates at the end of incubation and  
21 their PZC were measured in 1mM of KCl (pH  $\approx$  6.5). The result was consistent with previous  
22 zeta potential measurement and was approximately  $-20\pm 3$ mV. This test could not be  
23 successfully performed for cells attached to a hematite surface as sampling these cells was not  
24 feasible without removing the hematite coating deposited.

1           The AB10 medium is relatively high in ionic content and has an ionic strength (IS)  
2 value of 196.08 mM. Different studies show that increasing ionic strength leads to shrinkage  
3 of the diffuse double layer length around a charged colloidal particle, consequently hampering  
4 the effects of electrostatic interaction within a specific distance from the surface. Chen and  
5 Walker (2007)<sup>54</sup> showed that changing the ionic strength from 1 mM to 100 mM using KCl as  
6 the electrolyte caused considerable changes in bacterial cell surface potential. Considering this  
7 possibility, the zeta potential of Sph2 (planktonic) was measured in a suspension of AB10  
8 medium with lower levels of ionic strength. NaCl has the highest concentration in this medium  
9 (please see supporting information (SI)), and reducing the original ionic strength, from  
10 196.08mM to 98.8 mM and 19.06mM, was achieved by changing this electrolyte concentration  
11 in the AB10.

12           The results of this experiment are shown in Figure 8b. As seen, there was an  
13 approximately 20 mV difference between the measured zeta potential for a cell suspension in  
14 AB10 medium (identical to the attached growth experimental conditions) and an Sph2 cell  
15 suspension in 1mM of KCl. The cell surface charge was less negative and close to zero in the  
16 AB10 medium compared to 1mM of KCl. This result may explain the notable attachment of  
17 Sph2 to the polystyrene surface. The attraction forces due to electrostatic interactions might  
18 have made a negligible contribution to attachment, since the surface charge of the polystyrene  
19 and the effective surface charge of the bacterial strain were close to zero under the experiment's  
20 conditions. Therefore, attachment was probably governed by hydrophobicity. This case is  
21 supported by the fact that the outer cell-wall components of Sph2 are amphiphilic in nature,  
22 and this allows bacterial cells to attach and form a biofilm on a hydrophobic surface. This might  
23 also have been reinforced by the complexation of the charged groups on the outer cell wall  
24 macromolecules, due to the presence of positively charged ions in the AB10, leading to

1 conformational changes in the macromolecules. As a result, hydrophobic moieties might be  
2 more exposed to the ambient environment and facilitate adhesion to a hydrophobic surface.

3 This finding underlines the role of the growth medium's ionic strength. It also sheds  
4 light on the anomalies observed when studying Sph2 attachment to minerals and why cell-  
5 adhesion patterns are not consistent with the expected electrostatic attraction that should exist  
6 between Sph2 and metal-oxide surfaces. Considering the aforementioned facts, changing the  
7 ionic strength and consequently Sph2 surface potential should lead to different attachment  
8 behaviour. Reducing the ionic strength and altering the Sph2 surface potential (from close to  
9 neutral to  $\approx -20\text{mV}$ ) should cause a considerable increase in the number of cells attaching to  
10 positively charged metal oxides. Figure 9 shows the biofilm formation of Sph2 on a hematite  
11 surface in three different ionic strength conditions ( $\text{pH} = 6.5$ ). Figure 10 shows the numbers of  
12 Sph2 cells attached to a hematite surface after 96 hours of incubation at three different ionic  
13 strengths. As can be seen, when the ionic strength was reduced by a factor of ten, the number  
14 of the cells attached to the hematite increased approximately tenfold. The difference in Sph2  
15 surface potential under these two conditions is approximately  $-20\text{mV}$ , which reinforces the  
16 electrostatic attraction between positively charged hematite and a negatively charged Sph2  
17 surface.

18 In this research, biofilm formations on synthetic mineral surfaces of iron and aluminium  
19 oxides were studied under controlled laboratory conditions. The coating method, deposition of  
20 metal oxide colloidal particles from a suspension onto a cell-culture polystyrene surface,  
21 proved to be a simple but reliable approach for this purpose. This technique can be used in  
22 future studies to create multi-component surfaces that better represent the complexity of  
23 available mineral surfaces in nature. The novel imaging method developed for this research  
24 also indicates that direct, non-invasive and in situ imaging using a water-dipping objective and

1 Syto9 stain is a good alternative to crystal violet assay that is frequently used for studying  
2 biofilm formation.

3 The planktonic phase of environmental isolates suggest that these were not affected by  
4 the surface properties of hematite, goethite, aluminium hydroxide or model polystyrene.  
5 Planktonic-phase growth was better in the medium with a glucose-carbon source treatment  
6 compared to potassium acetate.

7 The experimental results suggest that cell-adhesion predictions based on the effects of  
8 electrostatic and hydrophobic interactions are likely to show discrepancies when compared to  
9 real attachment behaviour. In natural environments, the available surfaces for cell adhesion and  
10 biofilm formation, and the bacterial cell surface itself, are not pristine but affected by the ionic  
11 composition of the media, e.g. marine and groundwater environments. The dramatic increase  
12 in the number of Sph2 attached cells to the hematite surface, by changing the solution ionic  
13 strength, is a prime example of this effect; reducing the growth medium's ionic strength from  
14  $\approx 200$  mM to  $\approx 20$  mM resulted in ten times more attached cells

15 This research also demonstrates that the presence of a high number of bacterial cells in  
16 the planktonic phase does not necessarily represent extensive cell attachment and biofilm  
17 formation on surfaces. This finding is significant because in engineered bioremediation a high  
18 number of bacterial cells in the planktonic phase is often considered to be a good indication of  
19 the extent of biofilm formation in aquifers. The results suggest that when engineered solutions  
20 are planned, realistic predictions of bioremediation are only possible if the physicochemical  
21 properties of bacterial cells and mineral surfaces and the ionic strength of aquifer media are  
22 thoroughly characterized.

23

24

25

## 1 **Supporting information**

2 Supplementary data associated with this article can be found in the online version.  
3 Potentiometric titration of synthetic minerals, water-drop contact-angle measurements and  
4 XRD and FTIR spectra of synthetic minerals are available in this section. In addition, XPS  
5 spectra of the reference polystyrene and metal-oxide coated surfaces, details of the AB10  
6 growth medium's ionic content, the planktonic growth and biofilm formation of RC92, RC291,  
7 Pse1, Pse2, Sph1 and Sph2 bacterial strains when incubated under a KAc carbon source  
8 treatment are provided.

## 9 10 **References**

- 11
- 12 (1) Elliott, D. R.; Scholes, J. D.; Thornton, S. F.; Rizoulis, A.; Banwart, S. A.; Rolfe, S. A.  
13 Dynamic changes in microbial community structure and function in phenol-degrading  
14 microcosms inoculated with cells from a contaminated aquifer. *FEMS Microbiol Ecol* **2010**,  
15 *71* (2), 247–259.
- 16 (2) Fingerman, M. *Bioremediation of aquatic and terrestrial ecosystems*; CRC Press, 2016.
- 17 (3) Kanematsu, H.; Barry, D. M. Environmental Problems: Soil and Underground Water  
18 Treatment and Bioremediation. In *Biofilm and Materials Science*; Springer International  
19 Publishing: Cham, 2015; pp 117–123.
- 20 (4) Andrews, J. S.; Rolfe, S. A.; Huang, W. E.; Scholes, J. D.; Banwart, S. A. Biofilm formation  
21 in environmental bacteria is influenced by different macromolecules depending on genus and  
22 species. *Environ. Microbiol.* **2010**, *12*, 2496–2507.
- 23 (5) Ojeda, J. J.; Romero-Gonzalez, M. E.; Bachmann, R. T.; Edyvean, R. G. J.; Banwart, S. A.;  
24 Building, F. M.; Uni, T.; Street, M.; Sheffield, S.; Kingdom, U. Characterization of the cell  
25 surface and cell wall chemistry of drinking water bacteria by combining XPS, FTIR  
26 spectroscopy, modeling, and potentiometric titrations. *Langmuir* **2008**, *24* (8), 4032–4040.
- 27 (6) Karunakaran, E.; Mukherjee, J.; Ramalingam, B.; Biggs, C. A. “Biofilmology”: a  
28 multidisciplinary review of the study of microbial biofilms. *Appl. Microbiol. Biotechnol.* **2011**,  
29 *90* (6), 1869–1881.
- 30 (7) Salerno, M. B.; Logan, B. E.; Velegol, D. Importance of molecular details in predicting  
31 bacterial adhesion to hydrophobic surfaces. *Langmuir* **2004**, *20*, 10625–10629.
- 32 (8) Kwon, K. D.; Vellido-Rodriguez, V.; Logan, B. E.; Kubicki, J. D. Interactions of biopolymers  
33 with silica surfaces: Force measurements and electronic structure calculation studies.  
34 *Geochim. Cosmochim. Acta* **2006**, *70*, 3803–3819.
- 35 (9) Geoghegan, M.; Andrews, J. S.; Biggs, C. A.; Eboigbodin, K. E.; Elliott, D. R.; Rolfe, S.;  
36 Scholes, J.; Ojeda, J. J.; Romero-Gonzalez, M. E.; Edyvean, R. G. J.; et al. The polymer  
37 physics and chemistry of microbial cell attachment and adhesion. *Faraday Discuss* **2008**, *139*,  
38 28-85-420.
- 39 (10) Pouran, H. M.; Banwart, S. a.; Romero-Gonzales, M.; Romero-Gonzalez, M.; Romero-  
40 Gonzales, M. Coating a polystyrene well-plate surface with synthetic hematite, goethite and  
41 aluminium hydroxide for cell mineral adhesion studies in a controlled environment. *Appl.*  
42 *Geochemistry* **2014**, *42* (1986), 60–68.
- 43 (11) Rizoulis, A.; Elliott, D. R.; Rolfe, S. A.; Thornton, S. F.; Banwart, S. A.; Pickup, R. W.;  
44 Scholes, J. D. Diversity of planktonic and attached bacterial communities in a phenol-  
45 contaminated sandstone aquifer. *Microb Ecol* **2013**, *66* (1), 84–95.

- 1 (12) Crawford, R.; Webb, H.; Truong, V.; Hasan, J. Surface topographical factors influencing  
2 bacterial attachment. *Adv. colloid* **2012**.
- 3 (13) Zhang, X.; Zhang, Q.; Yan, T.; Jiang, Z. Quantitatively Predicting Bacterial Adhesion Using  
4 Surface Free Energy Determined with a Spectrophotometric Method. *Sci. Technol.* **2015**.
- 5 (14) Lyon, D.; Vogel, T. Bioaugmentation for groundwater remediation: an overview.  
6 *Bioaugmentation Groundw. Remediat.* **2013**.
- 7 (15) Scow, K. M.; Hicks, K. A. Natural attenuation and enhanced bioremediation of organic  
8 contaminants in groundwater. *Curr Opin Biotechnol* **2005**, *16* (3), 246–253.
- 9 (16) Shephard, J. J.; Savory, D. M.; Bremer, P. J.; McQuillan, A. J. Salt Modulates Bacterial  
10 Hydrophobicity and Charge Properties Influencing Adhesion of *Pseudomonas aeruginosa*  
11 (PA01) in Aqueous Suspensions. *Langmuir* **2010**, *26*, 8659–8665.
- 12 (17) and, L.-C. X.; Logan\*, B. E. Interaction Forces Measured Using AFM between Colloids and  
13 Surfaces Coated with Both Dextran and Protein. **2006**.
- 14 (18) Stumm, W.; Morgan, J. J. Aquatic chemistry, chemical equilibria and rates in natural waters.  
15 **1996**.
- 16 (19) Dixon, J. B.; Weed, S. B. Minerals in Soil Environment. *SSSA B. Ser.* **1992**.
- 17 (20) Huang, P. M.; Li, Y.; Sumner, M. E. (Malcolm E. . *Handbook of soil sciences : properties and*  
18 *processes*; CRC Press, 2012.
- 19 (21) Li, B.; Logan, B. E. Bacterial adhesion to glass and metal-oxide surfaces. **2004**, *36*, 81–90.
- 20 (22) Moradi, M.; Song, Z.; Nie, X.; Yan, M.; Hu, F. Q. Investigation of bacterial attachment and  
21 biofilm formation of two different *Pseudoalteromonas* species: Comparison of different  
22 methods. *Int. J. Adhes. Adhes.* **2016**, *65*, 70–78.
- 23 (23) Ojeda, J. J.; Romero-Gonzalez, M. E.; Pouran, H. M.; Banwart, S. a.; Romero-Gonzales, M.  
24 E.; Lane, B. In situ monitoring of the biofilm formation of *Pseudomonas putida* on hematite  
25 using flow-cell ATR-FTIR spectroscopy to investigate the formation of inner-sphere bonds  
26 between the bacteria and the mineral. *Mineral. Mag.* **2008**, *72* (1), 101–106.
- 27 (24) Claessens, J.; van Lith, Y.; Laverman, A. M.; Van Cappellen, P. Acid-base activity of live  
28 bacteria: Implications for quantifying cell wall charge. *Geochim. Cosmochim. Acta* **2006**, *70*,  
29 267–276.
- 30 (25) Lalonde, S. V.; Smith, D. S.; Owttrim, G. W.; Konhauser, K. O. Acid-base properties of  
31 cyanobacterial surfaces I: Influences of growth phase and nitrogen metabolism on cell surface  
32 reactivity. *Geochim. Cosmochim. Acta* **2008**, *72*, 1257–1268.
- 33 (26) Yee, N.; Benning, L. G.; Phoenix, V. R.; Ferris, F. G. Characterization of metal-cyanobacteria  
34 sorption reactions: A combined macroscopic and infrared spectroscopic investigation. *Env. Sci*  
35 *Technol* **2004**, *38*, 775–782.
- 36 (27) Vijayaraghavan, K.; Yun, Y. S. Bacterial biosorbents and biosorption. *Biotechnol. Adv.* **2008**,  
37 *26*, 266–291.
- 38 (28) Kapetas, L.; Ngwenya, B. T.; Macdonald, A. M.; Elphick, S. C. Kinetics of bacterial  
39 potentiometric titrations: The effect of equilibration time on buffering capacity of *Pantoea*  
40 *agglomerans* suspensions. *J. Colloid Interface Sci.* **2011**, *359*, 481–486.
- 41 (29) French, S.; Puddephatt, D.; Habash, M.; Glasauer, S. The dynamic nature of bacterial surfaces:  
42 Implications for metal–membrane interaction. *Crit. Rev. Microbiol.* **2013**, *39* (2), 196–217.
- 43 (30) Penners, N. H. G.; Koopal, L. K. Preparation And Optical-Properties Of Homodisperse  
44 Hematite Hydrosols. *Colloids And Surfaces* **1986**, *19*, 337–349.
- 45 (31) Schwertmann, U.; Cornell, R. M.; Wiley InterScience (Online service). *Iron oxides in the*  
46 *laboratory : preparation and characterization*; Wiley-VCH, 2008.
- 47 (32) Tang, B.; Ge, J. C.; Zhuo, L. H.; Wang, G. L.; Niu, J. Y.; Shi, Z. Q.; Dong, Y. B. A facile and  
48 controllable synthesis of gamma-Al<sub>2</sub>O<sub>3</sub> nanostructures without a surfactant. *Eur. J. Inorg.*  
49 *Chem.* **2005**, 4366–4369.
- 50 (33) Cornell, R. M.; Schwertmann, U. The Iron Oxides: Structure, Properties, Reactions,  
51 Occurrences and Uses Second, Completely Revised and Extended Edition. **2003**.
- 52 (34) Costanzo, P. M.; Wu, W.; Giese, R. F.; Vanoss, C. J. Comparison Between Direct-Contact  
53 Angle Measurements And Thin-Layer Wicking On Synthetic Monosized Cuboid Hematite  
54 Particles. *Langmuir* **1995**, *11*, 1827–1830.
- 55 (35) Costanzo, P. M.; Wu, W.; Giese, R. F. Comparison between Direct Contact Angle

- 1 Measurements and Thin Layer Wicking on Synthetic Monosized Cuboid Hematite Particles.  
2 **1996**, No. 7, 1827–1830.
- 3 (36) Lu, H. B.; Liao, L.; Li, J. C.; Shuai, M.; Liu, Y. L. Hematite nanochain networks: Simple  
4 synthesis, magnetic properties, and surface wettability. *Appl. Phys. Lett.* **2008**, *92*, 19–21.
- 5 (37) Förch, R.; Schönherr, H.; Jenkins, A. T. A. *Surface design : applications in bioscience and*  
6 *nanotechnology*; Wiley-VCH, 2009.
- 7 (38) Rosenberg, M.; Gutnick, D.; Rosenberg, E. Adherence Of Bacteria To Hydrocarbons - A  
8 Simple Method For Measuring Cell-Surface Hydrophobicity. *Fems Microbiol. Lett.* **1980**, *9*,  
9 29–33.
- 10 (39) Busscher, H. J.; Belt-Gritter, B. van de; Mei, H. C. van der. Implications of microbial adhesion  
11 to hydrocarbons for evaluating cell surface hydrophobicity - 1. Zeta potentials of hydrocarbon  
12 droplets. *Colloids Surfaces B Biointerfaces* **1995**, 3–4 (5), 111–116.
- 13 (40) Pablos, C.; van Grieken, R.; Marugán, J.; Chowdhury, I.; Walker, S. L. Study of bacterial  
14 adhesion onto immobilized TiO<sub>2</sub>: Effect on the photocatalytic activity for disinfection  
15 applications. *Catal. Today* **2013**, *209*, 140–146.
- 16 (41) CM0906, R2A Agar | Oxoid - Product Detail  
17 [http://www.oxoid.com/UK/blue/prod\\_detail/prod\\_detail.asp?pr=CM0906](http://www.oxoid.com/UK/blue/prod_detail/prod_detail.asp?pr=CM0906).
- 18 (42) Tolker-nielsen, T. I. M.; Brinch, U. C.; Ragas, P. C.; Andersen, J. B. O.; Jacobsen, C. S.;  
19 Molin, S. Development and dynamics of Pseudomonas sp biofilms. *J. Bacteriol.* **2000**, *182*  
20 (22), 6482–6489.
- 21 (43) Elliott, D. R.; Scholes, J. D.; Thornton, S. F.; Rizoulis, A.; Banwart, S. A.; Rolfe, S. A.  
22 Dynamic changes in microbial community structure and function in phenol-degrading  
23 microcosms inoculated with cells from a contaminated aquifer. *FEMS Microbiol. Ecol.* **2009**,  
24 *71* (2).
- 25 (44) Andrews, J. S.; Pوران, H. M.; Scholes, J.; Rolfe, S. A.; Banwart, S. A. Multi-factorial  
26 analysis of surface interactions in single species environmental bacteria and model surfaces.  
27 *Geochim. Cosmochim. Acta* **2009**, *73*, A44–A44.
- 28 (45) Acid, N.; Sampler, S. SYTO ® Green-Fluorescent Nucleic Acid Stains. **2008**, 33342, 1–7.
- 29 (46) Suwarno, S. R.; Hanada, S.; Chong, T. H.; Goto, S.; Henmi, M.; Fane, A. G. The effect of  
30 different surface conditioning layers on bacterial adhesion on reverse osmosis membranes.  
31 *Desalination* **2016**, *387*, 1–13.
- 32 (47) Falcon Polystyrene Microplates 12-well; Standard tissue culture; Flat-bottom;  
33 <https://www.fishersci.com/shop/products/falcon-tissue-culture-plates-12-well-standard-tissue-culture-flat-bottom-growth-area-3-8cm2-well-volume-6ml-1-tray/0877229>.
- 34 (48) Leone, L.; Ferri, D.; Manfredi, C.; Persson, P.; Shchukarev, A.; Sjöberg, S.; Loring, J.  
35 Modeling the acid-base properties of bacterial surfaces: A combined spectroscopic and  
36 potentiometric study of the gram-positive bacterium Bacillus subtilis. *Env. Sci Technol* **2007**,  
37 *41*, 6465–6471.
- 38 (49) Bouchez-Naitali, M.; Vandecasteele, J. P.; Vandecasteele, Æ. J.; Bouchez-nai, M.  
39 Biosurfactants, an help in the biodegradation of hexadecane? The case of Rhodococcus and  
40 Pseudomonas strains. *World J. Microbiol. Biotechnol.* **2008**, *24*, 1901–1907.
- 41 (50) Bouchez-nai, M.; Blanchet, D.; Bouchez-Naitali, M.; Blanchet, D.; Bardin, V.; Vandecasteele,  
42 J. P. Evidence for interfacial uptake in hexadecane degradation by Rhodococcus equi: the  
43 importance of cell flocculation. *Microbiology-Sgm* **2001**, *147*, 2537–2543.
- 44 (51) Huang, W.; Andrews, J.; Wang, Y. Ultrasonic DNA Transfer to Gram-Negative and Gram-  
45 Positive Bacteria. *Abstr. Gen. Meet. Am. Soc. Microbiol.* **2008**, *108*, 548.
- 46 (52) Kawahara, K.; Moll, H.; Knirel, Y. A.; Seydel, U.; Zahringer, U. Structural analysis of two  
47 glycosphingolipids from the lipopolysaccharide-lacking bacterium Sphingomonas capsulata.  
48 *Eur. J. Biochem.* **2000**, *267*, 1837–1846.
- 49 (53) Pruet, S. T.; Bushnev, A.; Hagedorn, K.; Adiga, M.; Haynes, C. A.; Sullards, M. C.; Liotta, D.  
50 C.; Merrill, A. H. Biodiversity of sphingoid bases (&quot;sphingosines&quot;) and related  
51 amino alcohols. *J. Lipid Res.* **2008**, *49* (8), 1621–1639.
- 52 (54) Chen, G. X.; Walker, S. L. Role of solution chemistry and ion valence on the adhesion kinetics  
53 of groundwater and marine bacteria. *Langmuir* **2007**, *23*, 7162–7169.
- 54  
55

1  
2  
3  
4  
5  
6  
7  
8  
9  
10  
11  
12  
13  
14  
15  
16  
17  
18  
19  
20  
21

## 1 **Legends to Figures**

2 **Figure 1.** Schematic representation of the main mechanisms involved in biofilm formation.

3 **Figure 2.** Schematic representation of incubating polystyrene and mineral-coated 12-well  
4 plates and directly imaging the strains attached to the studied surfaces. (a) Depicts confined  
5 lateral movements of the water-dipping objective due to the well's sides. As seen, a circle of  
6 diameter 11 mm located at the centre of each well's base was imaged for the studied substrata.  
7 (b) Shows direct imaging of the aluminium hydroxide-coated plates. (c) Illustrates the function  
8 of Z-height focusing, Z stacking, used in evaluating biofilm formation. This method was used  
9 for dense biofilms to better assess the numbers of cells attached to polystyrene and mineral  
10 surfaces.

11

12 **Figure 3.** Total numbers of cells in the planktonic phase for mineral-coated and reference  
13 polystyrene plates after 96 hours of incubation in AB10 medium with a glucose carbon source.

14

15 **Figure 4.** RC92 and RC291 attachments to mineral and polystyrene surfaces, a–d refer to RC92  
16 and e–h refer to RC291 adhesion to hematite, goethite, aluminium hydroxide and polystyrene,  
17 respectively (AB10 medium with glucose carbon sources, ionic strength = 196.08mM, pH=  
18 6.5).

19 **Figure 5.** Pse1 and Pse2 attachment to mineral and polystyrene surfaces, a–d refer to Pse1 and  
20 e–h refer to Pse2 adhesion to hematite, goethite, aluminium hydroxide and polystyrene,  
21 respectively (AB10 medium with glucose carbon sources, ionic strength = 196.08mM, pH=  
22 6.5).

23 **Figure 6.** Sph1 and Sph2 attachment to mineral and polystyrene surfaces, a–d refer to Sph1  
24 and e–h refer to Sph2 adhesion to hematite, goethite, aluminium hydroxide and polystyrene,  
25 respectively (AB10 medium with glucose carbon sources, ionic strength = 196.08mM, pH=  
26 6.5).

27 **Figure 7.** Total number of bacterial cells attached to mineral-coated polystyrene and  
28 polystyrene surfaces after 96 hours of incubation in AB10 medium with a glucose carbon  
29 source.

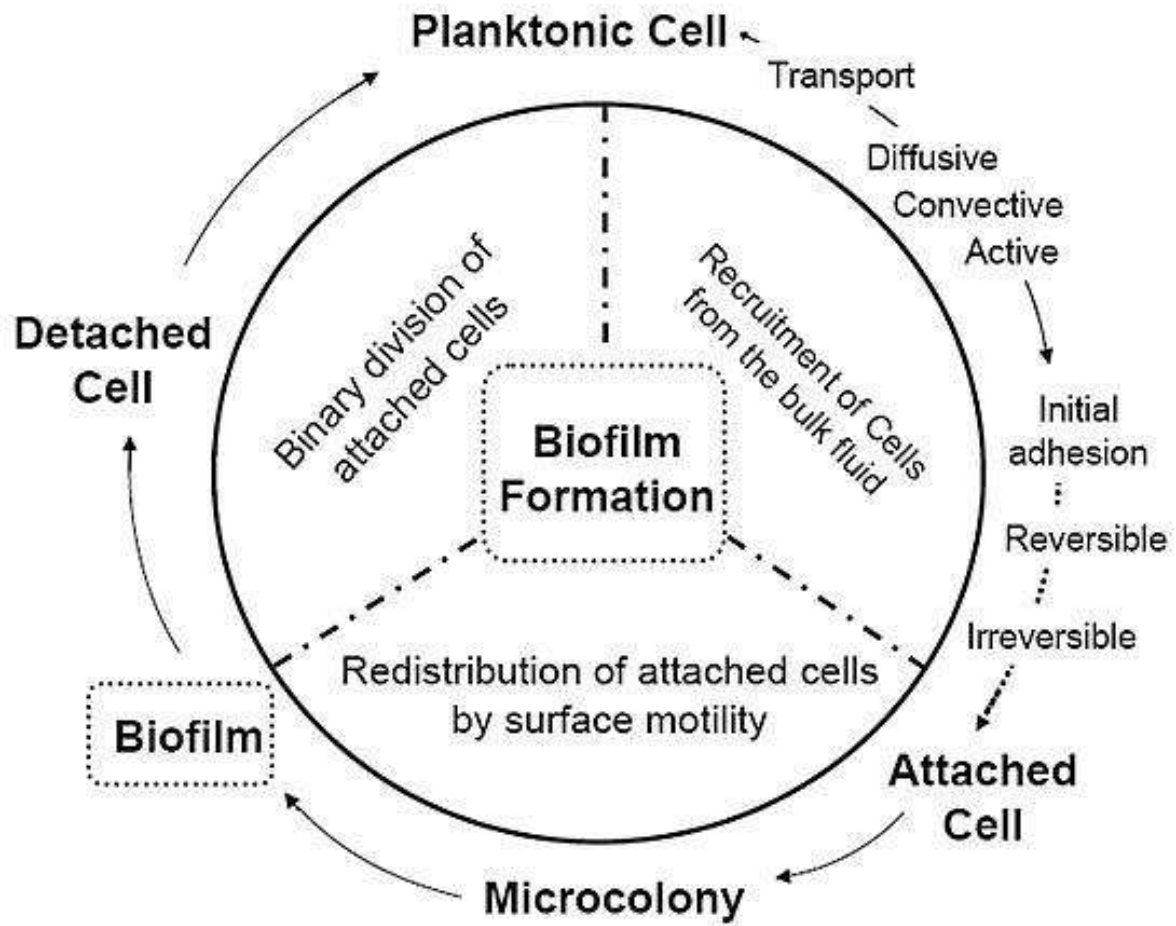
30 **Figure 8.** (a) Zeta potential of Sph2 strain suspended in 1 mM of KCl at different pH values.  
31 (b). Variations of the zeta potential of Sph2 strain in AB10 medium at different ionic strengths.

32 **Figure 9.** Attachment of Sph2 to a hematite surface under different ionic strengths (a; IS =196.08  
33 mM, b; IS = 98.08 mM, c; IS = 19.06 mM).

34 **Figure 10.** Quantified number of cells attached to hematite after 96 hours of incubation under  
35 different ionic strength (IS) conditions.

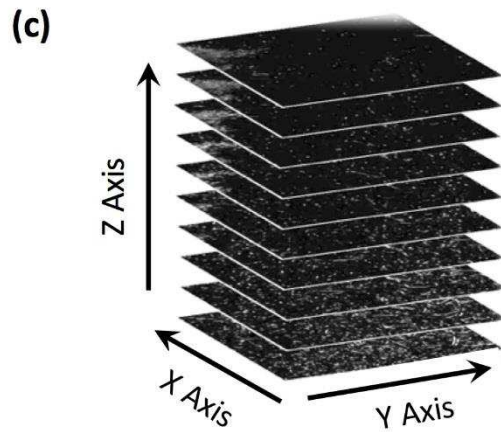
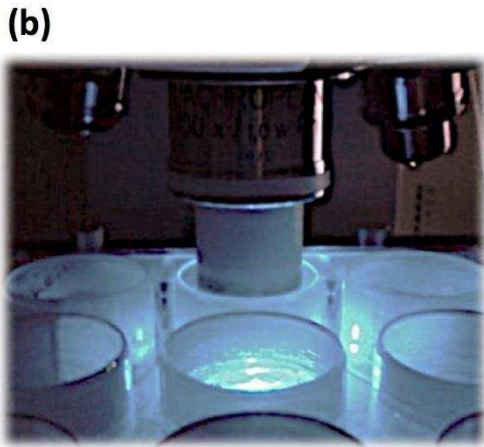
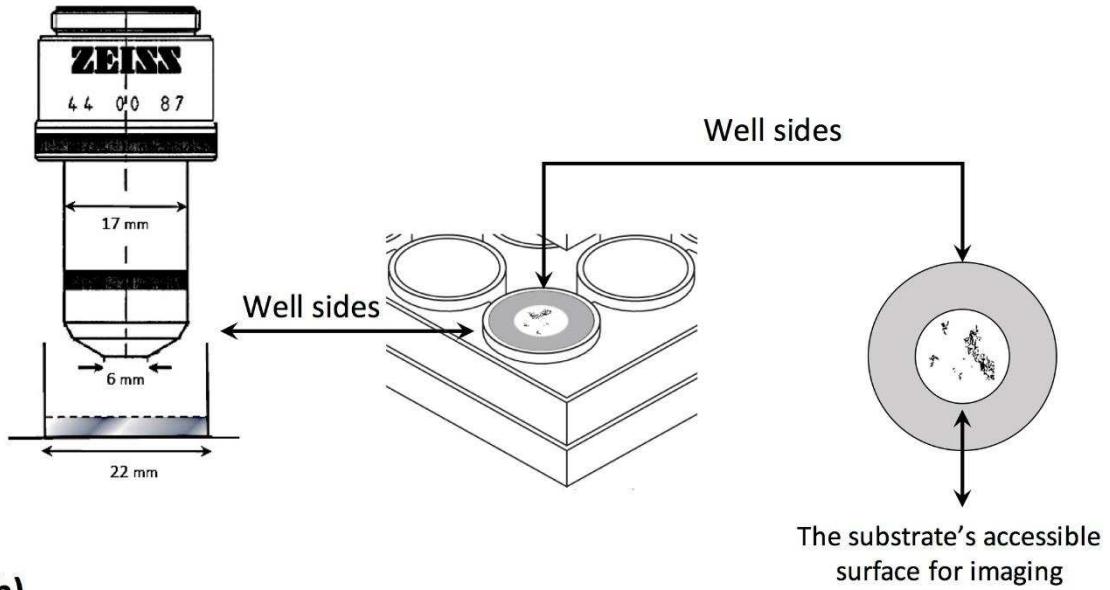
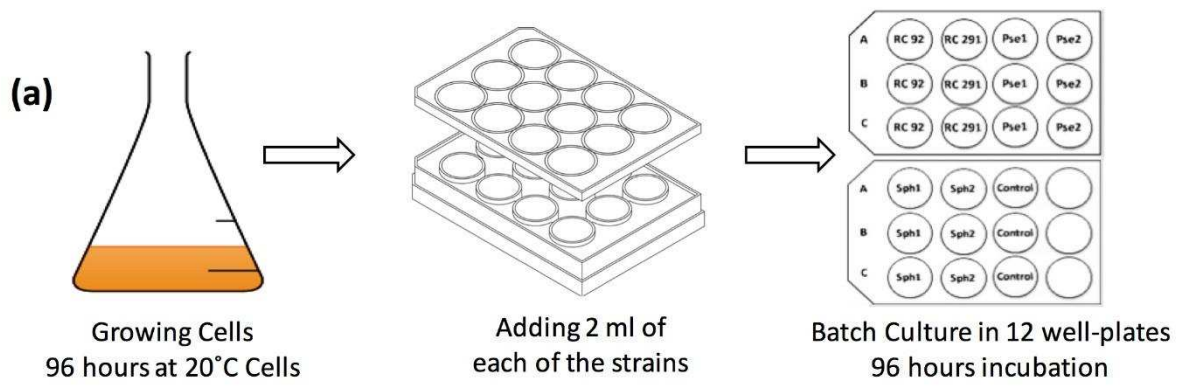
36 **Table 1.** Summarizes bacterial strains; RC92, RC291, Pse1, Pse2, Sph1 and Sph2 adhesion  
37 morphologies to polystyrene and mineral surfaces.

1  
2  
3



4  
5 **Figure 1**

6  
7  
8



1  
2 **Figure 2**

3

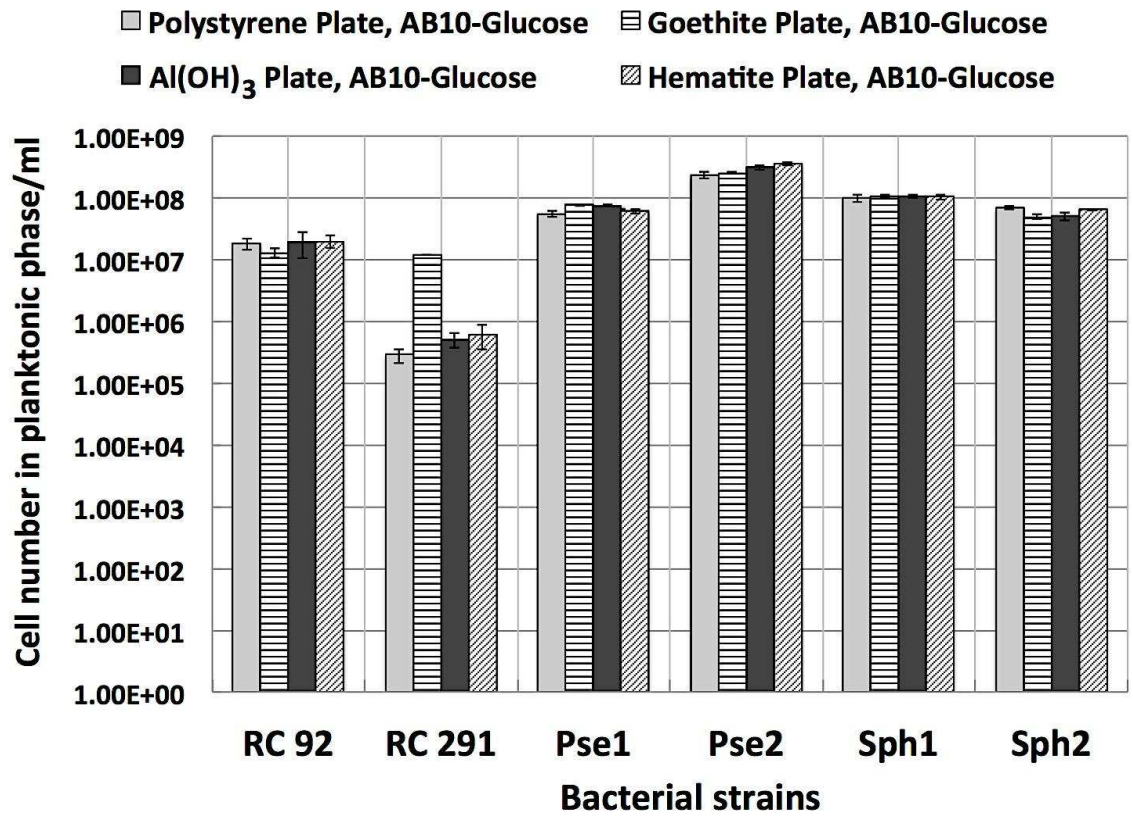
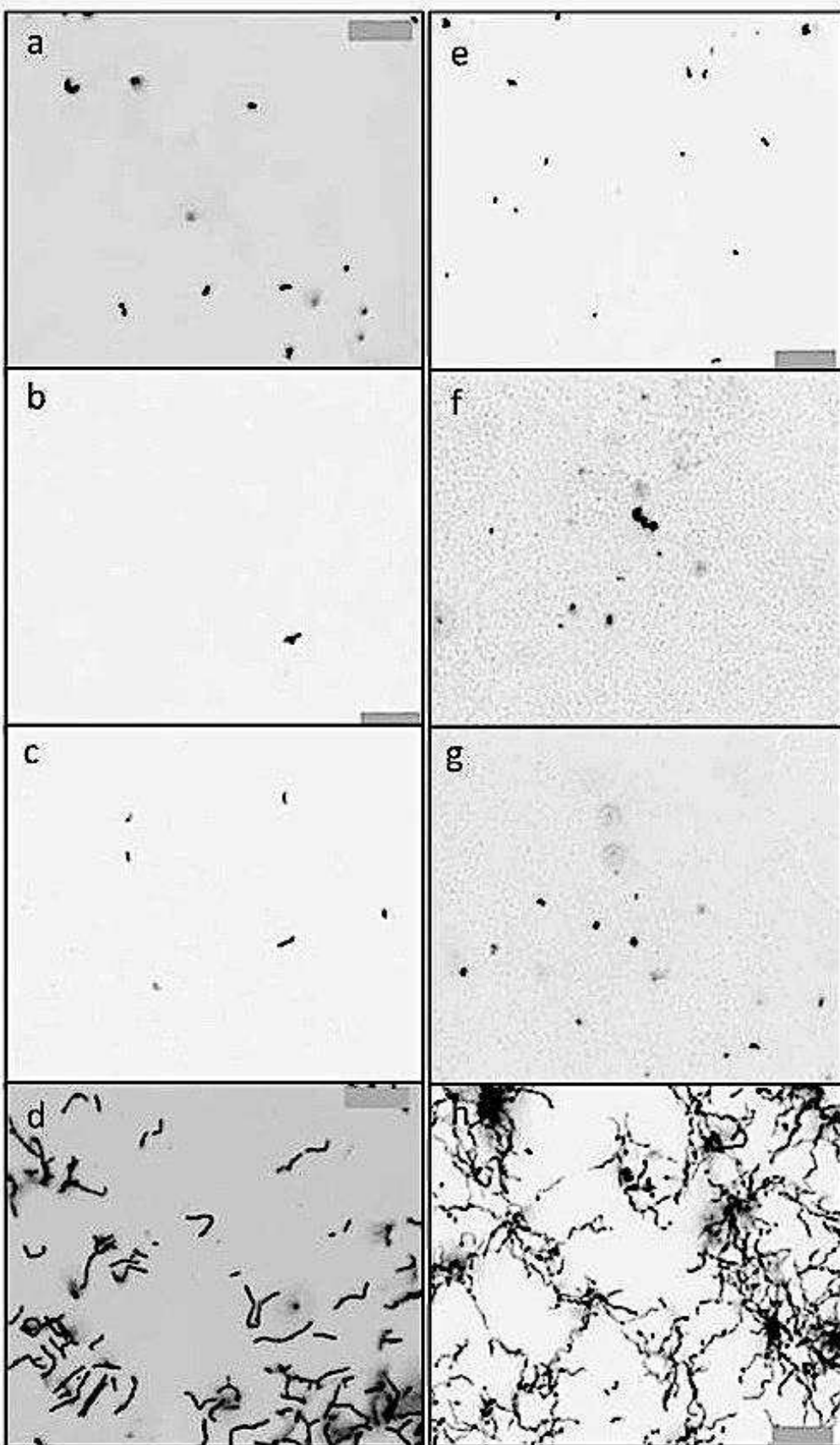


Figure 3

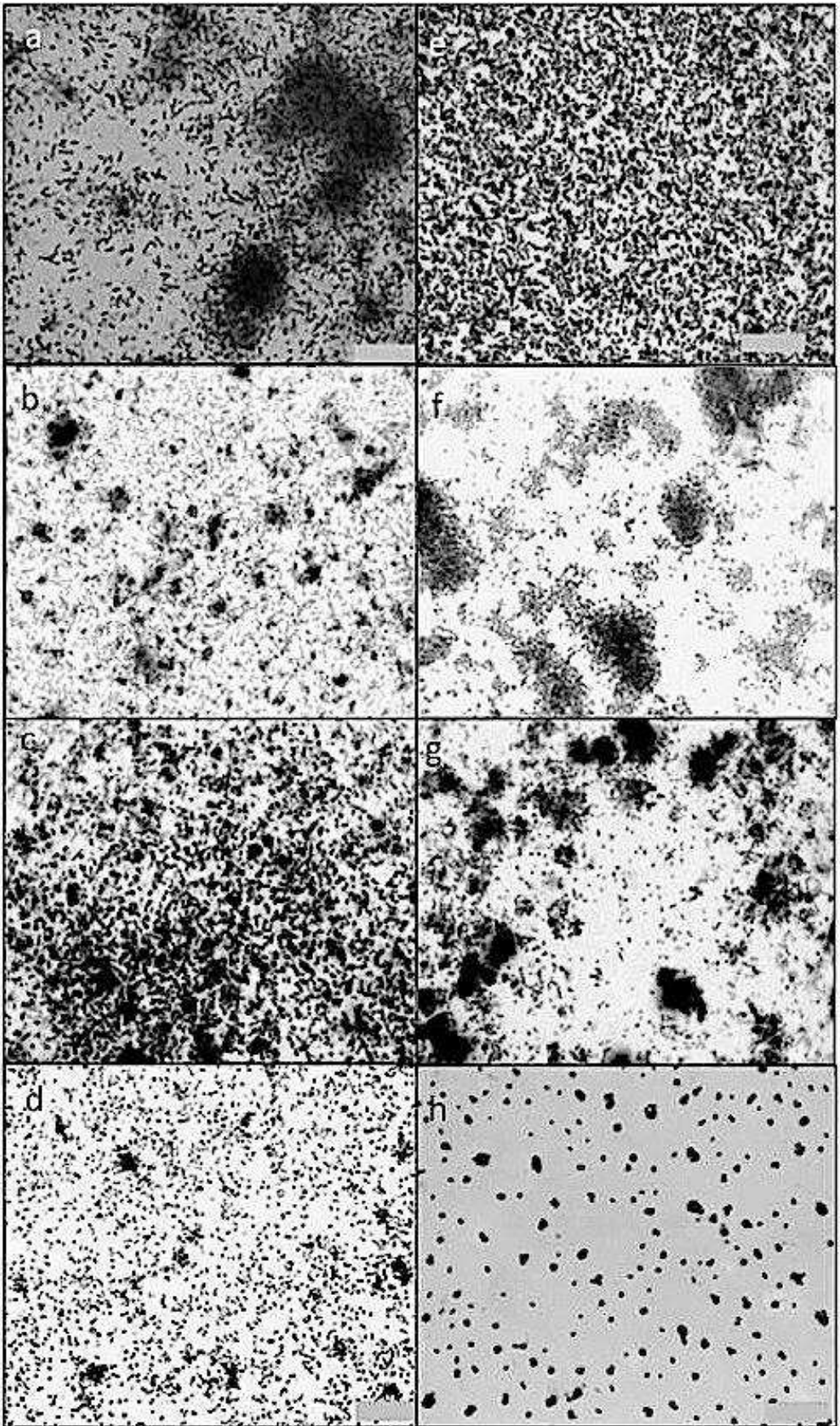
1  
2  
3  
4  
5  
6  
7  
8  
9  
10  
11  
12  
13  
14  
15  
16  
17  
18  
19  
20  
21  
22  
23  
24  
25  
26

1

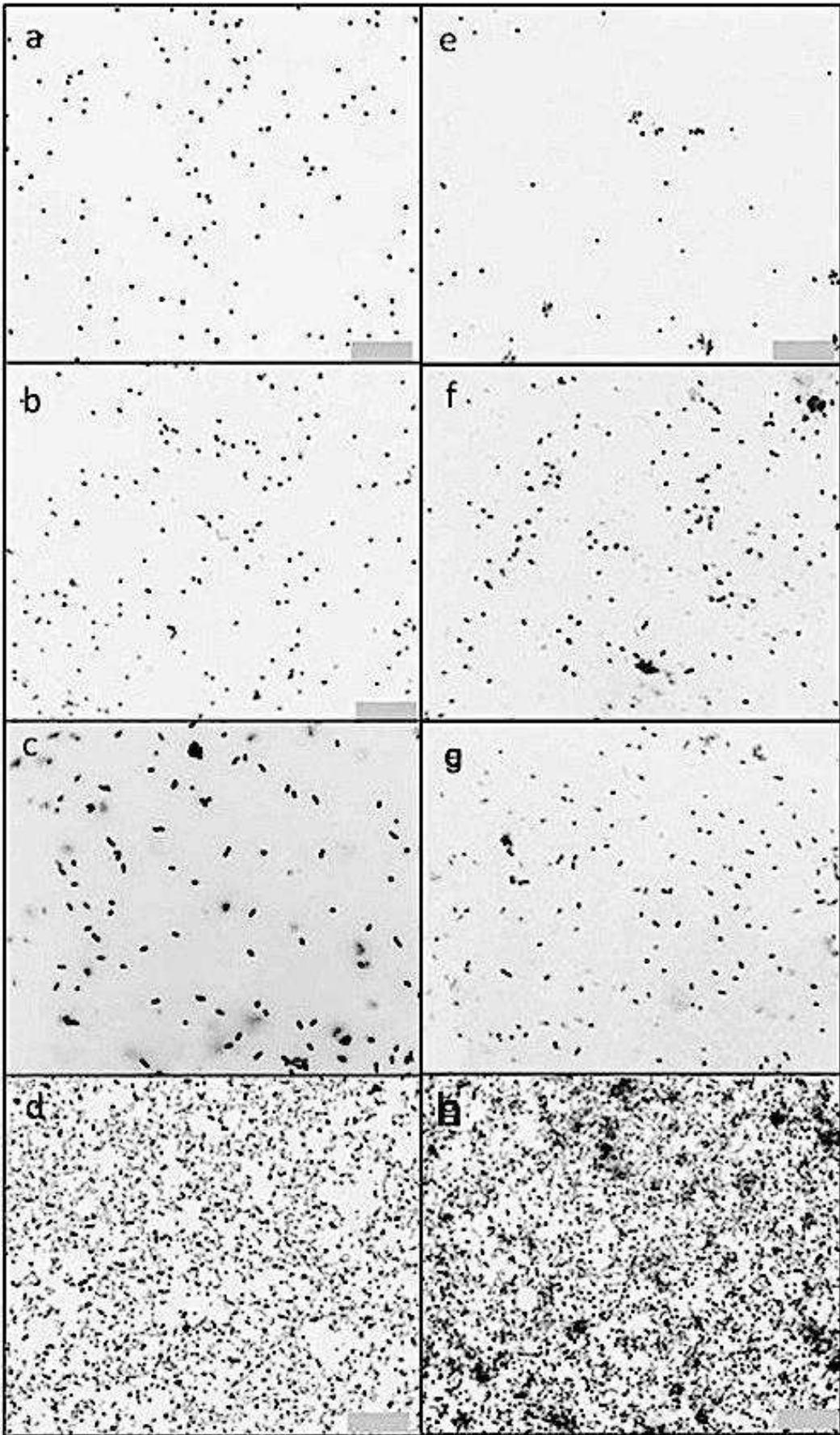


2  
3

**Figure 4**

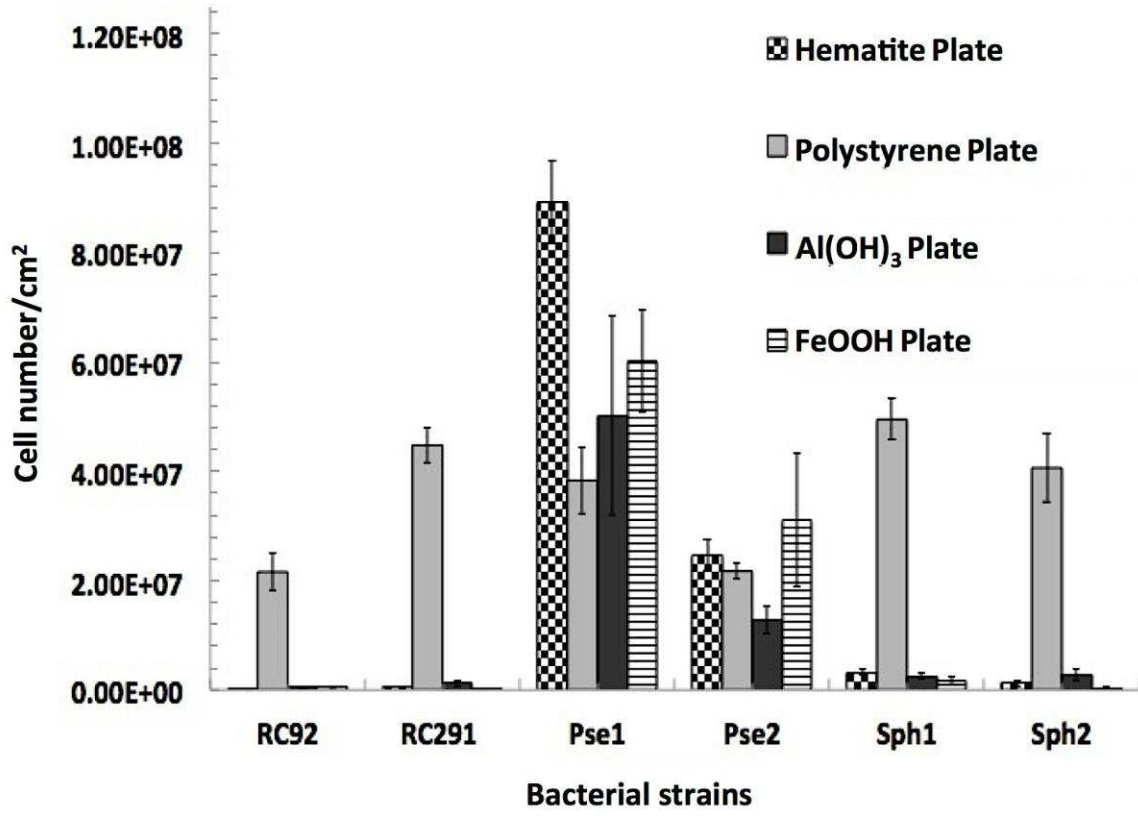


1  
2 **Figure 5**



1  
2 **Figure 6**

1



2

3

Figure 7

4

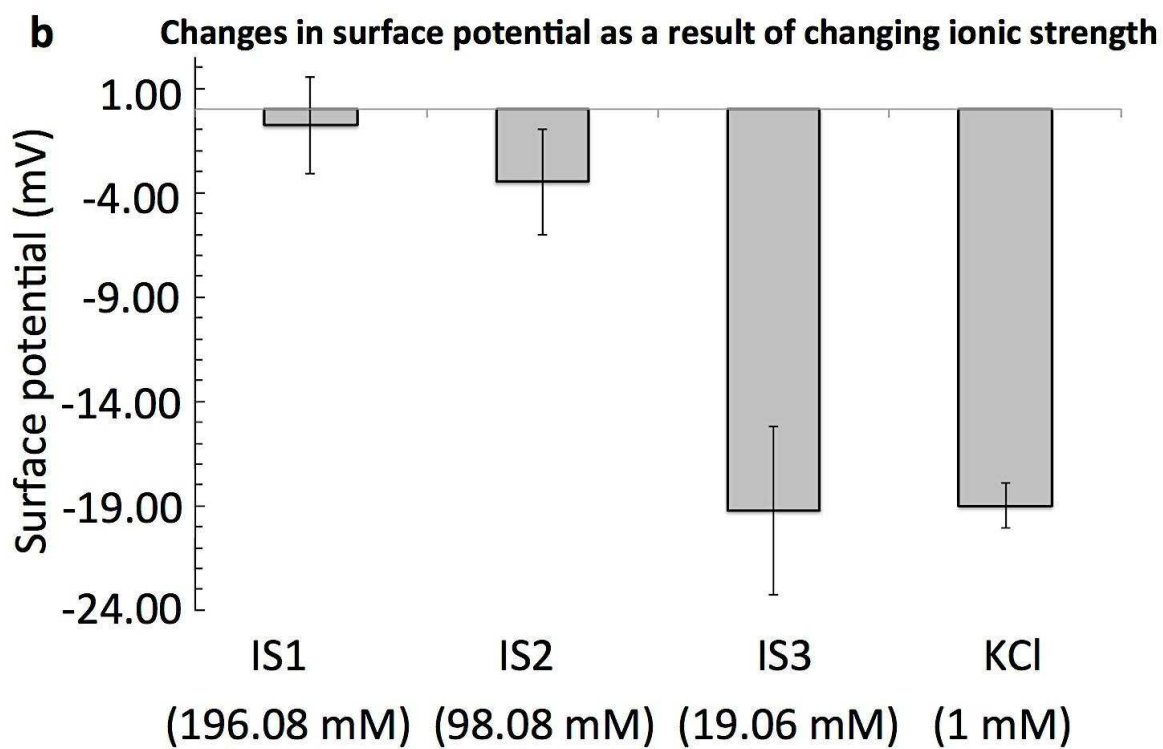
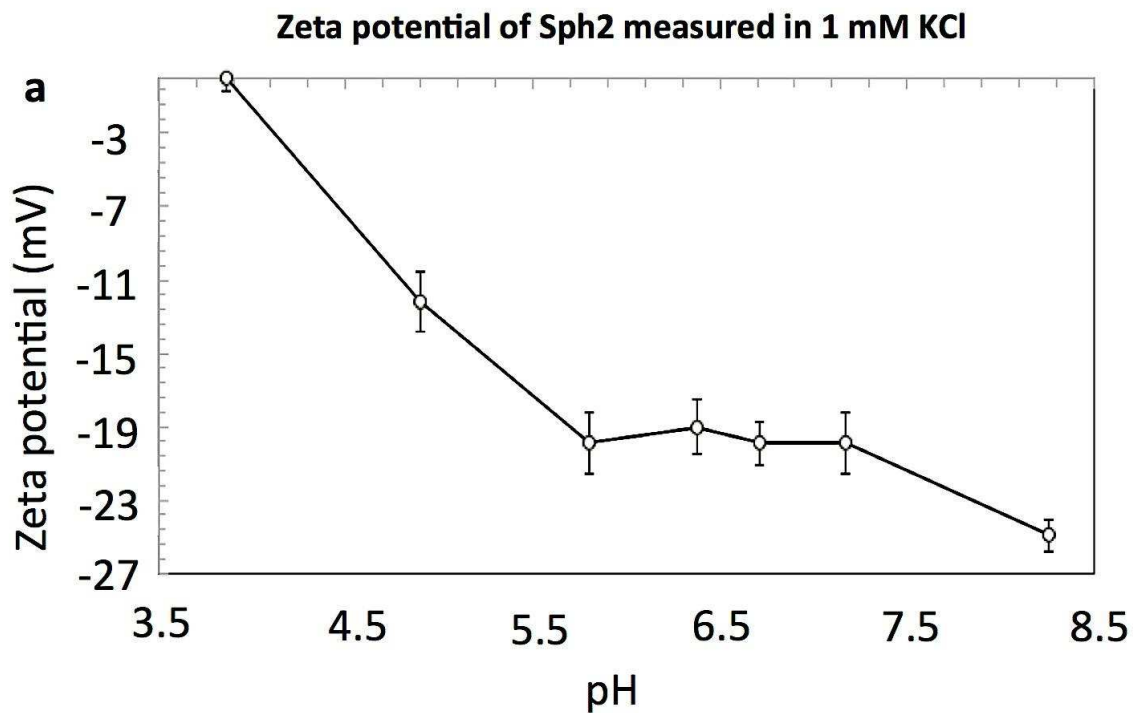
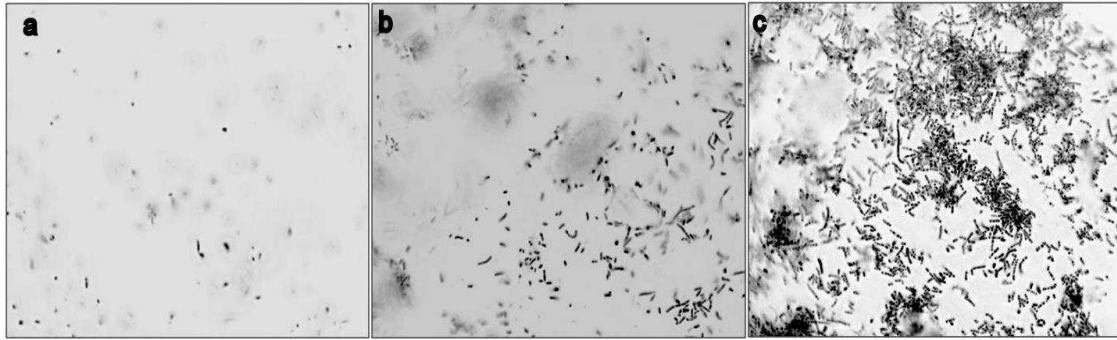


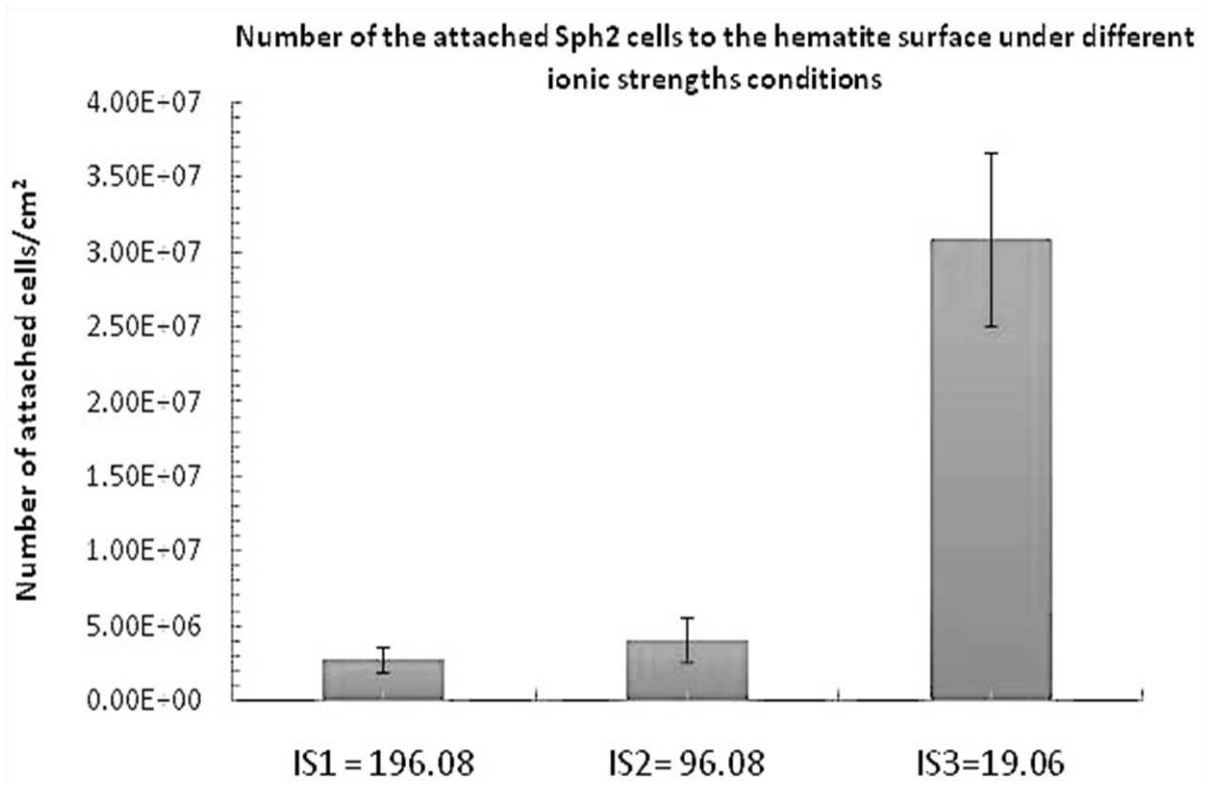
**Figure 8**

1  
2  
3  
4  
5  
6  
7  
8  
9



1  
2 **Figure 9**

3



4  
5 **Figure 10**

6

7

8

9

10

11

12

13

14

15

16

17

18

19

1  
2  
3  
4

**Table 1**

<b>Attachment Surface</b> <b>Bacterial Strain</b>	<b>Hematite Hydrophilic</b> <b>PZC=7.5</b>	<b>Goethite Hydrophilic</b> <b>PZC=8.5</b>	<b>Aluminum Hydroxide Hydrophilic</b> <b>PZC=8.9</b>	<b>Polystyrene Hydrophilic</b> <b>Neutral</b>
<b>RC92</b> <b>Hydrophobic, PZC&lt;6.5</b>	Negligible cell attachment	Negligible cell attachment	Negligible cell attachment	Dispersed chain-shape biofilm
<b>RC291</b> <b>Hydrophobic, PZC&lt;6.5</b>	Negligible cell attachment	Negligible cell attachment	Negligible cell attachment	Highly structured biofilm
<b>Pse1</b> <b>Hydrophilic, PZC&lt;6.5</b>	Extensive cell clusters	Extensive cell clusters	Extensive cell clusters	Sparse micro-colonies
<b>Pse2</b> <b>Hydrophilic, PZC&lt;6.5</b>	Extensive cell clusters	Extensive cell clusters	Extensive cell clusters	Sparse micro-colonies
<b>Sph1</b> <b>Hydrophobic, PZC&lt;6.5</b>	Poor, dispersed single-cell attachment	Poor, dispersed single-cell attachment	Poor, dispersed single-cell attachment	Extensive cell attachment
<b>Sph2</b> <b>Hydrophilic, PZC&lt;6.5</b>	Poor, dispersed single-cell attachment	Poor, dispersed single-cell attachment	Poor, dispersed single-cell attachment	Extensive cell attachment

5  
6  
7